

ω -3 PUFAs Attenuate Postoperative Ileus by Modulating Macrophage Polarization via the JAK2/STAT3 Signaling Pathway

Xuan Zhao^{1,*}, Jing Yu^{1,*}, Tianle Zhang¹, Yufei Zhang¹, Liuchuang Zhang¹, Ye Wang¹, Chen Yi¹, Huafeng Pan², Haifeng Wang², Miaomiao Ge², Zhiwei Jiang², Gang Wang²

¹Affiliated Hospital of Nanjing University of Chinese Medicine, Nanjing, Jiangsu, People's Republic of China; ²Department of General Surgery, Jiangsu Province Hospital of Chinese Medicine, Affiliated Hospital of Nanjing University of Chinese Medicine, Nanjing, Jiangsu, People's Republic of China

*These authors contributed equally to this work

Correspondence: Gang Wang; Zhiwei Jiang, Email gwang82@163.com; surgery34@163.com

Objective: This study explored the therapeutic effects and mechanisms of omega-3 polyunsaturated fatty acids (ω -3 PUFAs) on postoperative ileus (POI) and their potential in preventing or treating POI.

Methods: A murine model of postoperative ileus (POI) and an in vitro macrophage inflammation model were employed. Analyses included the assessment of intestinal injury, motility, inflammatory cytokines, macrophage infiltration, and polarization. RNA sequencing implicated the JAK2/STAT3 pathway, which was validated through immunohistochemistry and Western blot. Subsequent STAT3 knockout and overexpression experiments in macrophages further elucidated the underlying mechanism.

Results: ω -3 PUFAs alleviated intestinal damage, restored motility, and reduced local pro-inflammatory cytokine levels in POI mice, along with reduced macrophage infiltration. In vitro, ω -3 PUFAs suppressed M1 polarization. RNA-seq implicated the JAK/STAT pathway, and further experiments confirmed that ω -3 PUFAs markedly suppressed the phosphorylation of JAK2, STAT3, and p65 in both macrophages and ileal tissue. Genetic manipulation of STAT3 established that ω -3 PUFAs attenuate inflammation primarily through modulating macrophage polarization.

Conclusion: ω -3 PUFAs alleviate POI by inhibiting the JAK2/STAT3 signaling pathway in macrophages, thereby suppressing their polarization toward the pro-inflammatory M1 phenotype and reducing local intestinal inflammation. These findings indicate that ω -3 PUFAs may be a promising prophylactic or therapeutic agent for POI.

Keywords: omega-3 polyunsaturated fatty acids, postoperative ileus, macrophage polarization, inflammatory cytokines, JAK2/STAT3 signaling pathway

Introduction

Postoperative ileus (POI) refers to an impairment in gastrointestinal motility that frequently arises after abdominal procedures. This condition is characterized by clinical features such as abdominal pain, bloating, nausea, vomiting, oral intolerance, and difficulty in passing stool or gas, which collectively impair postoperative recovery and quality of life.¹⁻³ In recent decades, Enhanced Recovery After Surgery (ERAS) protocols have reduced postoperative complications and markedly improved patient outcomes.^{4,5} Current clinical practice relies primarily on ERAS-based perioperative care, supplemented by adjuncts such as gum chewing, electroacupuncture, and prokinetics to promote bowel recovery. However, once POI is established, evidence-based specific therapeutics remain lacking, and management remains largely supportive and multimodal.⁶ Thus, POI persists as a prevalent complication following abdominal surgery.⁷ Epidemiological data indicate that POI occurs in 10%–30% of cases in the United States, incurring annual healthcare costs of roughly \$1.47 billion.⁸⁻¹⁰ Therefore, reducing the incidence of POI is critical for improving patient prognosis and lowering healthcare costs.

The pathogenesis of POI involves neurogenic and inflammatory phases.^{11,12} In particular, intestinal inflammation driven by macrophages is central to the pathogenesis of POI.¹³ Surgical manipulation or trauma induces the polarization of gastrointestinal macrophages into the pro-inflammatory M1 phenotype. These activated macrophages subsequently secrete inflammatory mediators, including IL-1 β , IL-6, and TNF- α . These cytokines and mast cell degranulation promote neutrophil recruitment and establish a positive feedback cycle that escalates localized inflammation and compromises the contractile function of gastrointestinal smooth muscle.^{14,15} The JAK/STAT signaling pathway is a key regulator of macrophage polarization.^{16,17} External stimuli induce the phosphorylation of JAK1 and JAK2, activating STAT1 and STAT3 transcription factors, which drive M1 macrophage polarization and inflammatory cytokine production.¹⁸ Hence, modulating macrophage polarization presents a promising POI prevention and treatment strategy.

Omega-3 polyunsaturated fatty acids (ω -3 PUFAs) are essential for human physiological function and are primarily derived from two sources: deep-sea organisms, which provide abundant eicosapentaenoic acid (EPA) and docosahexaenoic acid (DHA), and terrestrial plants, which are rich in α -linolenic acid (ALA).^{19,20} Accumulating evidence indicates that EPA and DHA exert significant anti-inflammatory properties, as evidenced by their ability to inhibit the secretion of key cytokines from macrophages. Furthermore, these fatty acids are thought to modulate macrophage polarization through modifications in lipid and energy metabolic pathways.^{21–23} Preliminary clinical studies have found that enteral supplementation with ω -3 PUFAs can attenuate intestinal inflammation and promote bowel recovery after surgery without elevating postoperative complications, supporting their potential as a therapeutic option for POI, while the underlying mechanisms remain unclear.^{24,25} Whether ω -3 PUFAs exert these protective effects by specifically modulating the JAK2/STAT3 signaling pathway in macrophages remains unexplored. Elucidating this mechanism could provide a novel molecular basis for their therapeutic application in POI. This study therefore examined this mechanism in a murine POI model to establish a theoretical foundation for clinical translation.

Materials and Methods

Materials

The ω -3 PUFAs used in this study were commercially sourced from Nanjing Duly Biotech Co., Ltd. (Nanjing, China). EPA (#E2011) and DHA (#D2534) were obtained from Sigma-Aldrich (St. Louis, MO, USA). Antibodies against p-JAK2 (#8082), JAK2 (#3230), p-STAT3 (#9145), STAT3 (#4904), p-p65 (#3033), and p65 (#8242) were purchased from Cell Signaling Technology (CST) (Danvers, MA, USA). The antibody against α -SMA (#124964) was acquired from Abcam. Antibodies targeting p-MLC (29504-1-AP), MLC (10906-1-AP), GAPDH (60004-1-Ig), as well as mouse (RGAM001) and rabbit (RGAR001) secondary antibodies, were procured from Proteintech Group, Inc. (Wuhan, China). ELISA kits for the inflammatory cytokines IL-1 β and TNF- α were purchased from Epizyme Biomedical Technology Co., Ltd. (Shanghai, China), and the IL-6 ELISA kit was obtained from Elabscience Biotechnology Co., Ltd. (Wuhan, China). The fluorescently labeled antibody FITC-conjugated anti-CD86 was sourced from BD Biosciences (Shanghai, China), and PE-conjugated anti-CD206 was purchased from BioLegend (San Diego, CA, USA).

Animal Experiments

SPF male C57BL/6 mice, aged 8 weeks and weighing 23–25 g, were acquired from Zhejiang Vital River Laboratory Animal Technology Co., Ltd. (License No. SCXK(Zhe) 2020–0002). The animals were maintained in a controlled environment (22 \pm 2°C, 50 \pm 10% humidity, 12-hour light/dark cycle) with ad libitum access to food and water, and were acclimated for 1 week. All experimental protocols were reviewed and approved by the Ethics Committee of the Affiliated Hospital of Nanjing University of Chinese Medicine (Approval No. 2024DW-075-01) and performed in compliance with the ARRIVE 2.0 guidelines ([Supplementary Material 1](#)).

To establish the POI model, mice were subjected to a 12-hour fast and 6-hour water deprivation before anesthesia induction with 1.5–2.0% isoflurane. After abdominal disinfection, a 2-cm midline laparotomy was performed to allow visualization and access to the small intestine. For POI induction, the intestinal tract was carefully positioned on sterile moist gauze and subjected to gentle manipulation using a sterile cotton applicator along the extent from the Treitz ligament to the ileocecal junction for 10 minutes, inducing congestion and edema. The intestine was subsequently repositioned into the abdominal cavity, and the incision was sutured. Sham-operated animals received the same surgical

procedure excluding intestinal manipulation. Postoperatively, mice were maintained on a heating pad until full recovery of consciousness and then returned to their cages.

The mice were randomly assigned to four experimental groups, with ten animals in each group: Sham, POI, ω 3-L, and ω 3-H. Immediately after surgery, Sham and POI mice received 0.2 mL saline by oral gavage twice daily. Mice in the ω 3-L and ω 3-H groups were given low-dose (0.14 g/kg) and high-dose (0.28 g/kg) fish oil emulsions containing ω -3 PUFAs. The emulsion was delivered orally at a volume of 100 μ L per 10 g of body weight, twice a day for two consecutive days. Twelve hours after the final dose, mice were euthanized by cervical dislocation. Ileal segments were harvested, cleared of luminal contents, and subsequently either immersion-fixed in 4% paraformaldehyde or flash-frozen in liquid nitrogen for preservation at -80°C pending further analysis.

Cell Culture and Treatment

The cellular model employed in this research was the RAW 264.7 murine macrophage line, obtained from the Stem Cell Bank of the Chinese Academy of Sciences (Shanghai). The cells were cultured in DMEM supplemented with 10% FBS. To induce polarization into the pro-inflammatory M1 phenotype under in vitro conditions, macrophages were stimulated for 24 hours using a combination of 100 ng/mL LPS and 20 ng/mL IFN- γ . Owing to the lipophilic properties of EPA and DHA, both compounds were initially solubilized in DMSO to produce 100 mM stock solutions for use in further experiments. The study comprised four experimental conditions: a blank control group, a M1 induction group (LPS+IFN- γ), a solvent control group (LPS+IFN- γ +DMSO), and an ω 3 treatment group (LPS+IFN- γ +EPA+DHA).

Lentiviral Transduction

RAW 264.7 cells were transduced with a STAT3- overexpressing lentiviral vector (STAT3-TK-PCDH-copGFP-T2A-Puro) or its corresponding control. For STAT3 knockout, cells were transduced with LentiCRISPRv2Puro carrying STAT3-targeting sgRNA (sg-STAT3) or a non-targeting control (sg-NC). Following puromycin selection (2 μ g/mL, 7–10 days), successful genetic manipulation was confirmed by qRT-PCR and Western blot.

Assessment of Gastrointestinal Motility

The charcoal transit test assessed gastrointestinal motility. Twelve hours after the last treatment, mice received an oral gavage of a 10% activated charcoal suspension prepared in 10% gum Arabic, administered at a volume of 100 μ L per 10 g of body weight. After an additional 15 minutes, the mice were euthanized by cervical dislocation, and the complete small intestine was excised. The overall length of the intestine and the propagation distance of the charcoal bolus were then determined. Intestinal transit was expressed as the percentage of the distance traversed by the charcoal relative to the total intestinal length.

Histopathological Analysis (H&E Staining)

Segments of ileal tissue (approximately 0.5 cm in length) were immersion-fixed in 4% paraformaldehyde. Subsequently, the samples were processed through a graded ethanol series for dehydration, followed by embedding in paraffin wax. Thin sections were then prepared from the embedded blocks and subjected to H&E staining. An investigator blinded to group assignments examined histopathological changes in the ileum under a light microscope.

Enzyme-Linked Immunosorbent Assay (ELISA)

The concentrations of IL-1 β , IL-6, and TNF- α in ileal homogenates and cell culture supernatants were quantified using specific commercial ELISA kits, in strict accordance with the manufacturers' protocols. The absorbance for each sample was measured at the specified wavelength with a microplate reader.

Quantitative Real-Time PCR (qRT-PCR)

Total RNA was isolated from ileal tissues or RAW 264.7 cells with TRIzol reagent, following the supplier's recommended procedures. cDNA was generated through reverse transcription using a commercial kit. qRT-PCR was carried out with SYBR Green Master Mix on a real-time PCR instrument. The primer sequences for the target genes and the reference gene are provided in Table 1. Relative expression levels of the target genes were calculated using the $2^{-\Delta\Delta\text{Ct}}$ method.

Table 1 Primer Sequences for qRT-PCR Analysis

Gene	Forward Primer (5'→3')	Reverse Primer (5'→3')	Amplicon (bp)
IL-1 β	GCCTGTGTTTCCTCCTTGC	TGCTGCCTAATGTCCCCTTG	108
IL-6	AGACAAAGCCAGAGTCCTTCAG	TGTGACTCCAGCTTATCTCTTGG	77
TNF- α	CGGGCAGGTCTACTTTGGAG	ACCCTGAGCCATAATCCCCT	166
GAPDH	GCAAATTC AACGGCACAGTCAAG	TCGCTCCTGGAAGATGGTGATG	80

Immunohistochemistry and Immunofluorescence

Paraffin-embedded ileal sections underwent dewaxing and antigen retrieval in citrate buffer prior to immunohistochemical staining. Endogenous peroxidase activity was quenched, and non-specific binding sites were blocked with goat serum. The sections were then incubated at 4°C overnight with primary antibodies targeting p-JAK2, p-STAT3 or p-p65. After washing, HRP-conjugated secondary antibodies were applied. Color development was achieved using DAB substrate, and nuclei were counterstained with hematoxylin.

For immunofluorescence staining, frozen ileal sections were first fixed and permeabilized using 0.2% Triton X-100, then incubated with 5% BSA to block non-specific binding. The sections were probed overnight at 4°C with an anti-F4/80 antibody—a widely used macrophage marker—for macrophage identification. After washing, the sections were incubated with fluorescently-labeled secondary antibodies for 30 minutes at room temperature under light-protected conditions. Cell nuclei were stained with DAPI for nuclear visualization. Finally, the slides were mounted and imaged using a fluorescence microscope. Quantification of macrophage infiltration was performed by counting F4/80-positive cells.

Cell Viability Assay

RAW 264.7 cells were evenly seeded in 96-well plates at an appropriate density and cultured for 24 hours. Following this, the cells were exposed to various concentrations of EPA (0–500 μ M) or DHA (0–250 μ M), which were prepared in DMSO, for an additional 24-hour period. Viability was determined following the manufacturer's protocol for the CCK-8 kit.

RNA Sequencing (RNA-Seq)

RAW264.7 cells were grouped into CON, M1, and ω 3. Total RNA was extracted using TRIzol, and transcriptome sequencing was performed on the Illumina Novaseq™ 6000 platform by LC-Bio Technology Co., Ltd. (Hangzhou, China). After quality control with fastp, transcript assembly and quantification were conducted using StringTie. Differential expression analysis was performed in R with edgeR, with DEGs defined as $Q < 0.05$ and $|\log_2FC| > 1$. Subsequent analyses included expression profiling and functional enrichment.

Flow Cytometry for Macrophage Polarization

To analyze macrophage polarization, cells were first washed twice with pre-cooled PBS buffer, then incubated with an anti-CD86 antibody at 4°C for 30 minutes protected from light. After two additional washes, the cells were fixed and permeabilized, followed by incubation with an anti-CD206 antibody at 4°C for 30 minutes. Following another wash, the samples were analyzed by flow cytometry. Data were processed with FlowJo software, and macrophages were categorized as M1 (CD86⁺) or M2 (CD206⁺) based on surface marker expression.

Western Blotting

Ileal tissues or RAW 264.7 cells were lysed in RIPA buffer. Protein concentration was determined by BCA assay. Proteins were separated by electrophoresis on 10% or 12.5% SDS-PAGE gels and subsequently transferred onto PVDF membranes. The membranes were then blocked with 5% BSA solution at room temperature for 1 hour, followed by incubation with primary antibodies overnight. After washing, membranes were incubated with HRP-conjugated secondary antibodies for one hour and developed using an enhanced chemiluminescence system (Tanon, China).

Statistical Analysis

Statistical analyses were performed using GraphPad Prism 9.0. Differences between multiple groups were analyzed by one-way analysis of variance (ANOVA) followed by Tukey's post hoc test. $P < 0.05$ was considered statistically significant. All data collection and analysis were conducted under blinded conditions to minimize subjective bias.

Results

ω -3 PUFAs Ameliorate POI Symptoms

In the POI model, ω -3 PUFAs treatment improved clinical and histological outcomes. 48 hours after surgery, mice in the ω 3-L and ω 3-H groups lost significantly less body weight than the POI group (Figure 1A). The charcoal transit test showed that POI mice had markedly reduced intestinal transit compared to sham, whereas ω -3 PUFAs dose-dependently restored gastrointestinal motility (Figure 1B and C). Concurrently, protein expression levels of α -SMA, p-MLC and MLC were reduced in the POI group, indicating impaired intestinal contractility. Treatment with ω -3 PUFAs resulted in increased expression of these proteins (Figure 1D and E). Histological examination of the ileum revealed intact villus architecture and minimal inflammation in Sham mice. In contrast, POI mice showed severe mucosal damage, including epithelial sloughing, exposed lamina propria, inflammatory cell infiltration, and vascular congestion/edema. These pathological changes were markedly attenuated in both ω 3-L and ω 3-H groups (Figure 1F).

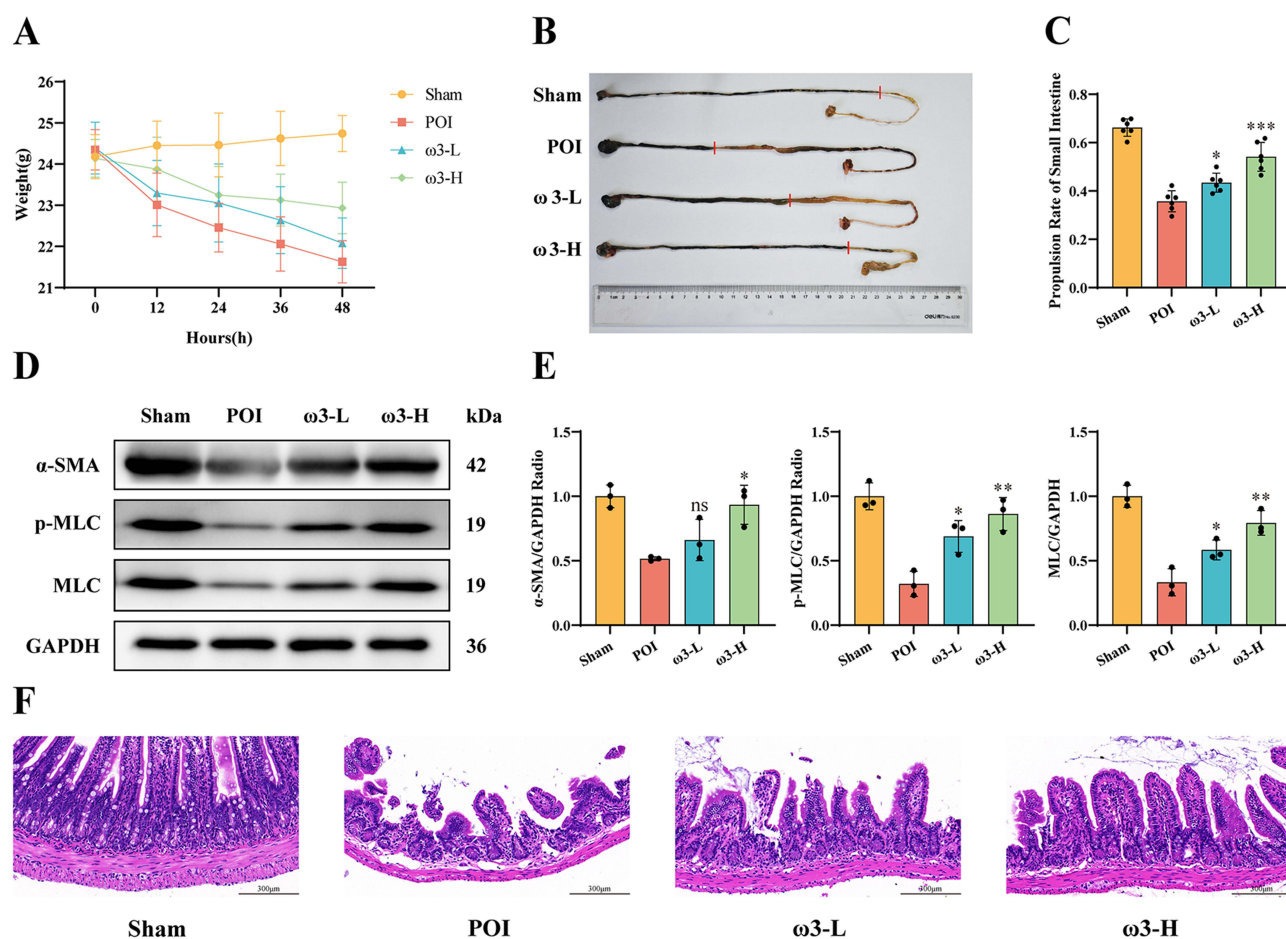


Figure 1 ω -3 PUFAs ameliorate intestinal injury in mice with postoperative ileus. (A) Body weight changes in different experimental groups following surgical intervention (n=10). (B and C) Distance traveled by charcoal front and charcoal transit ratio were calculated in different experimental groups. The red line indicates the leading edge of charcoal movement in the small intestine. (n = 6). (D and E) Expression levels of α -SMA, p-MLC, and MLC proteins in the small intestine in different groups (n = 3). (F) Representative H&E-stained sections depicting ileal tissue morphology in different groups (n = 6). Scale bar: 300 μ m. * $P < 0.05$, ** $P < 0.01$, *** $P < 0.001$, ns (not significant) vs POI group.

ω -3 PUFAs Reduce Intestinal Macrophage Infiltration and Suppress Local Inflammation

We next examined intestinal inflammation. Immunofluorescence staining with an anti-F4/80 antibody, a general macrophage marker, demonstrated a notable elevation in macrophage infiltration within the ileal tissue of POI mice relative to Sham, which was significantly reduced by ω -3 PUFAs treatment in both ω 3-L and ω 3-H groups (Figure 2A and B). ELISA confirmed that ω -3 PUFAs treatment reduced IL-1 β , IL-6 and TNF- α protein levels in ileal tissue homogenates (Figure 2C). In parallel, qRT-PCR showed that IL-1 β , IL-6 and TNF- α mRNA were upregulated in POI mice, and ω -3

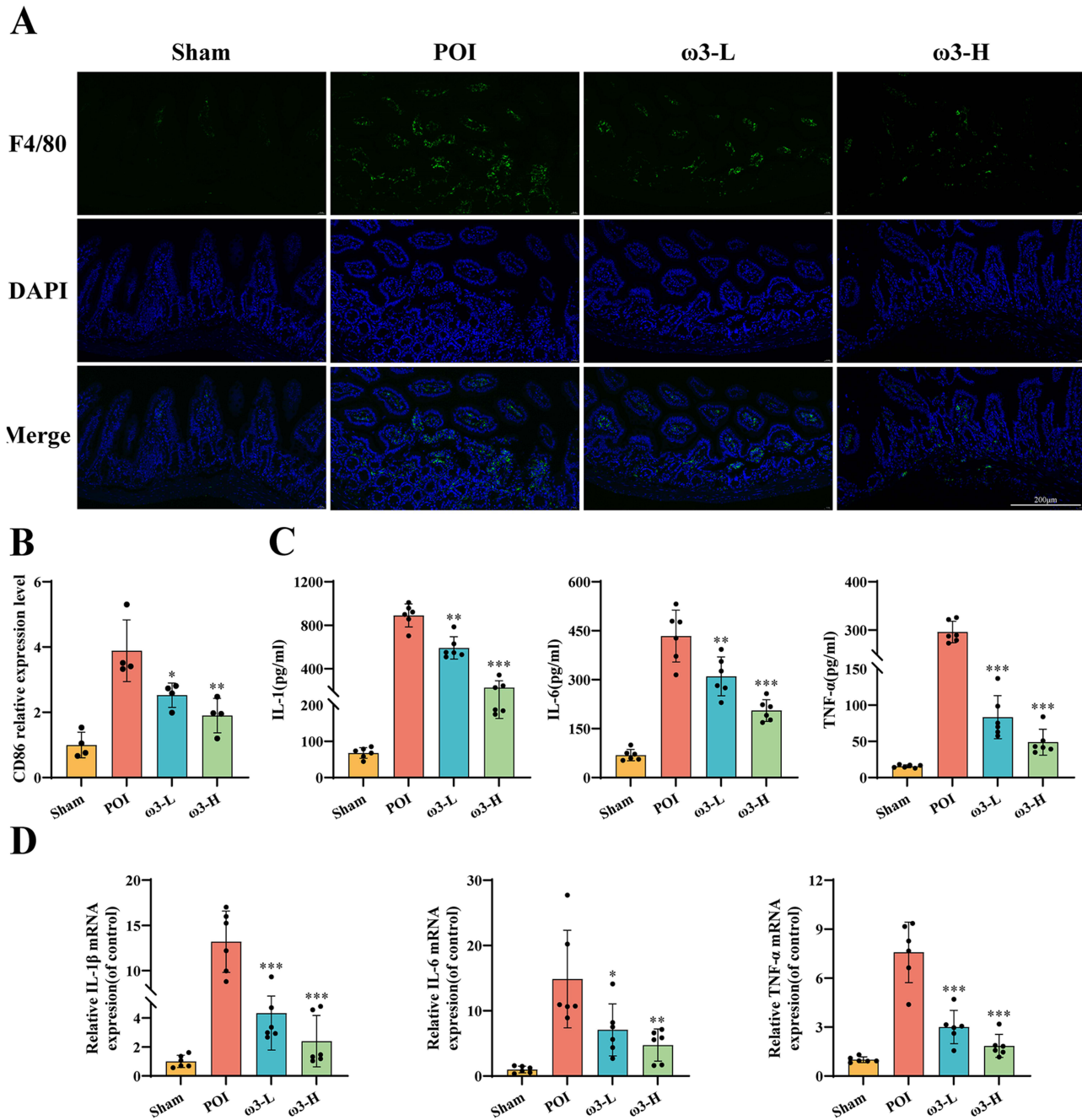


Figure 2 ω -3 PUFAs reduce macrophage infiltration and pro-inflammatory cytokine levels in the ileum of POI mice. (A and B) Infiltration of F4/80⁺ macrophages in ileal tissue was detected by immunofluorescence staining. (n = 4). Scale bar: 200 μ m. (C) Levels of pro-inflammatory cytokines (IL-1 β , IL-6 TNF- α) in ileal tissue homogenates measured by ELISA (n = 6). (D) mRNA expression levels of IL-1 β , IL-6 and TNF- α in ileal tissues determined by qRT-PCR (n = 6). *P < 0.05, **P < 0.01, ***P < 0.001 vs POI group.

PUFAs dose-dependently decreased their expression, especially in the ω 3-H group (Figure 2D). These findings demonstrate that ω -3 PUFAs mitigate intestinal inflammation in POI by limiting macrophage infiltration and suppressing pro-inflammatory cytokine production.

ω -3 PUFAs Inhibit M1 Macrophage Polarization and Pro-Inflammatory Cytokine Secretion *in vitro*

We treated RAW 264.7 cells with ω -3 PUFAs under inflammatory conditions to investigate the direct effects on macrophages. CCK-8 assays showed that 100 μ M EPA and 50 μ M DHA did not affect cell viability after 24 h (Figure 3A). Flow cytometry demonstrated that ω -3 PUFAs treatments significantly reduced the expression of the M1 marker CD86 induced by LPS+IFN- γ , with no significant effect on the M2 marker CD206 (Figure 3B and C). Both ELISA and qRT-PCR analyses demonstrated that ω -3 PUFAs markedly reduced the LPS+IFN- γ -induced production and release of IL-1 β , IL-6, and TNF- α (Figure 3D and E). These findings suggest that ω -3 PUFAs suppress the polarization of macrophages into the pro-inflammatory M1 subtype and reduce the secretion of major inflammatory cytokines.

Transcriptomic Profiling Implicates JAK2-STAT3 Signaling in ω -3 PUFA Action

We performed RNA-seq on CON, M1 and ω 3 group macrophages to identify underlying mechanisms. The PCA confirmed distinct transcriptomic profiles for each group (Figure 4A). Differential expression analysis revealed 9,390 DEGs between control and M1 (4,746 upregulated, 4,644 downregulated; Figure 4B) and 5,961 DEGs between M1 and ω 3-treated cells (2,906 upregulated, 3,055 downregulated; Figure 4C). The intersection of these two sets yielded 4,553 common genes (Figure 4D). KEGG pathway enrichment and GSEA plot analysis revealed activation of the JAK/STAT pathway in M1 group macrophages (Figure 4E and G), whereas the expression of genes associated with this pathway was down-regulated in the ω 3 group (Figure 4F–H). Comparative analysis across the three groups indicated elevated expression of JAK2 and STAT3 in the M1 group, which was attenuated following ω -3 PUFAs treatment (Figure 4I). These results indicate that ω -3 PUFAs may act by modulating the JAK2/STAT3 signaling pathway.

ω -3 PUFAs Suppress JAK2/STAT3 Phosphorylation *in vitro* and *in vivo*

We next examined JAK2/STAT3 signaling. Western blot analysis of LPS+IFN- γ -stimulated macrophages confirmed robust phosphorylation of JAK2, STAT3 and p65 in the M1 group. ω -3 PUFA treatment markedly suppressed phosphorylation of all three proteins (Figure 5A and B). Similarly, in ileal tissue from POI mice, immunohistochemistry and Western blotting showed elevated p-JAK2, p-STAT3, and p-p65 compared to Sham. Treatment with ω -3 PUFAs (ω 3-L and ω 3-H) dose-dependently reduced phosphorylation of these signaling molecules (Figure 5C and D). These data indicate that POI involves activation of the JAK2/STAT3 axis and that ω -3 PUFAs inhibit this pathway *in vivo* and *in vitro*.

STAT3 Knockout Synergizes with ω -3 PUFAs to Inhibit M1 Polarization

To confirm the role of STAT3, we generated STAT3 knockout (STAT3-KO) RAW 264.7 cells using CRISPR/Cas9. Western blot verified loss of total and phosphorylated STAT3 (Figure 6A and B). Flow cytometry showed that STAT3-KO alone significantly reduced LPS+IFN- γ -induced CD86 expression. Combining STAT3 knockout with ω -3 PUFA treatment nearly abolished CD86 expression (Figure 6C and D). Similarly, STAT3-KO significantly decreased secreted protein (Figure 6E) and mRNA (Figure 6F) levels of IL-1 β , IL-6 and TNF- α , and ω -3 PUFAs further enhanced this suppression. These findings confirm that STAT3 is a critical regulator of M1 polarization and cytokine production and that its inhibition synergizes with ω -3 PUFAs.

STAT3 Overexpression Partially Reverses the Anti-Inflammatory Action of ω -3 PUFAs

We then overexpressed STAT3 in RAW 264.7 cells. Western blot confirmed successful STAT3 overexpression and increased STAT3 phosphorylation (Figure 7A and B). STAT3-OE significantly enhanced LPS+IFN- γ -induced CD86 expression compared to vector control. Critically, STAT3-OE reduced the ability of ω -3 PUFAs to suppress CD86 expression (Figure 7C and D). Moreover, STAT3-OE increased protein and mRNA levels of IL-1 β , IL-6 and TNF- α ,

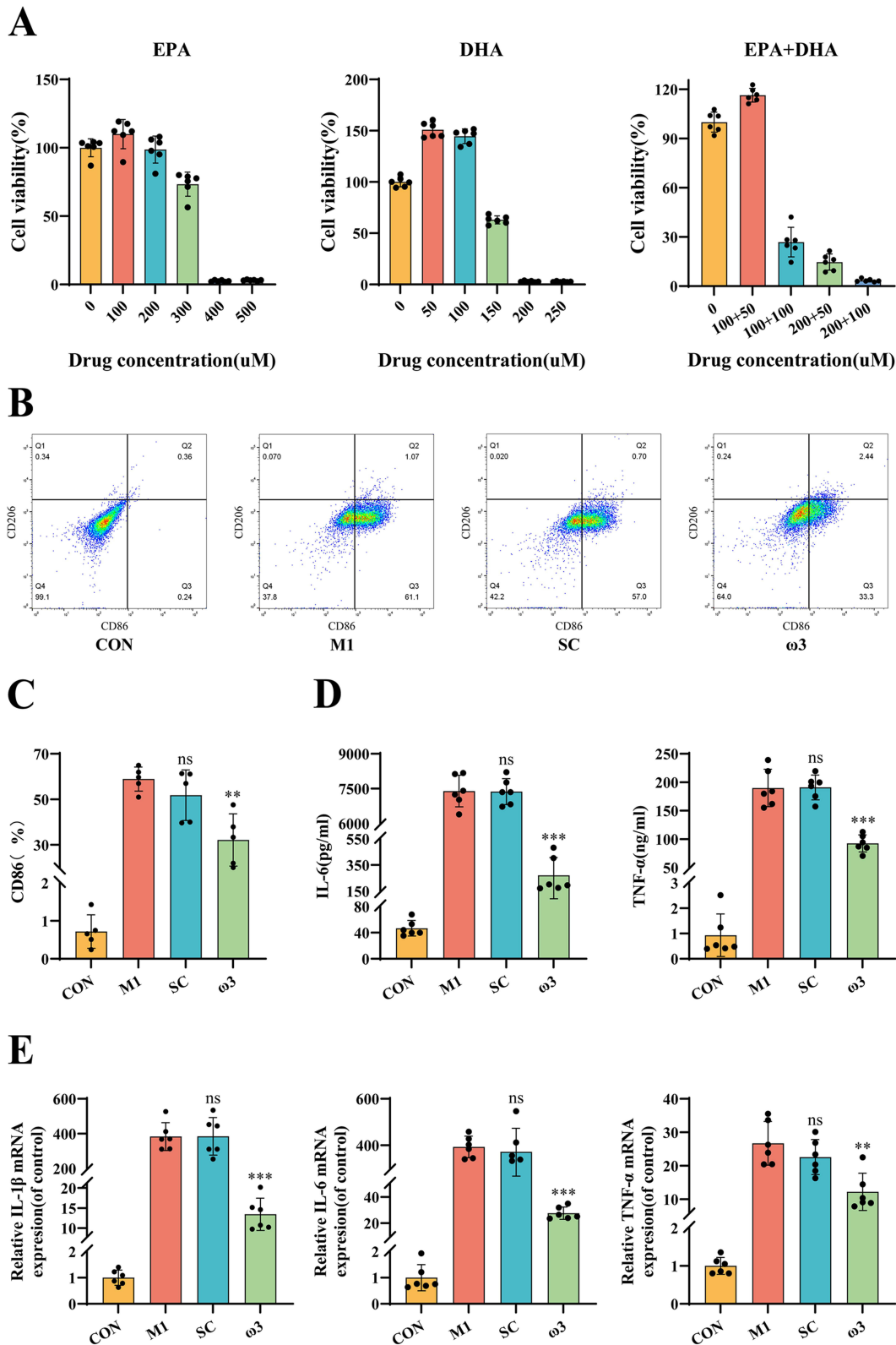


Figure 3 ω-3 PUFAs inhibit M1 macrophage polarization and reduce pro-inflammatory cytokine levels. **(A)** Cell viability of RAW 264.7 macrophages treated with varying concentrations of EPA or DHA for 24 hours, assessed by CCK-8 assay. Concentrations of 100 μM EPA and 50 μM DHA (used in subsequent experiments) showed no significant cytotoxicity. **(B and C)** Flow cytometry analysis of macrophage polarization. Representative flow cytometry plots gated on live cells showing CD86 (M1 marker) vs CD206 (M2 marker) expression. (n = 5). **(D)** Levels of IL-6 and TNF-α in cell culture supernatants measured by ELISA (n = 6). **(E)** mRNA expression levels of IL-1β, IL-6, and TNF-α in RAW 264.7 cells determined by qRT-PCR (n = 6). *P < 0.05, **P < 0.01, ***P < 0.001, ns (not significant) vs M1 group.

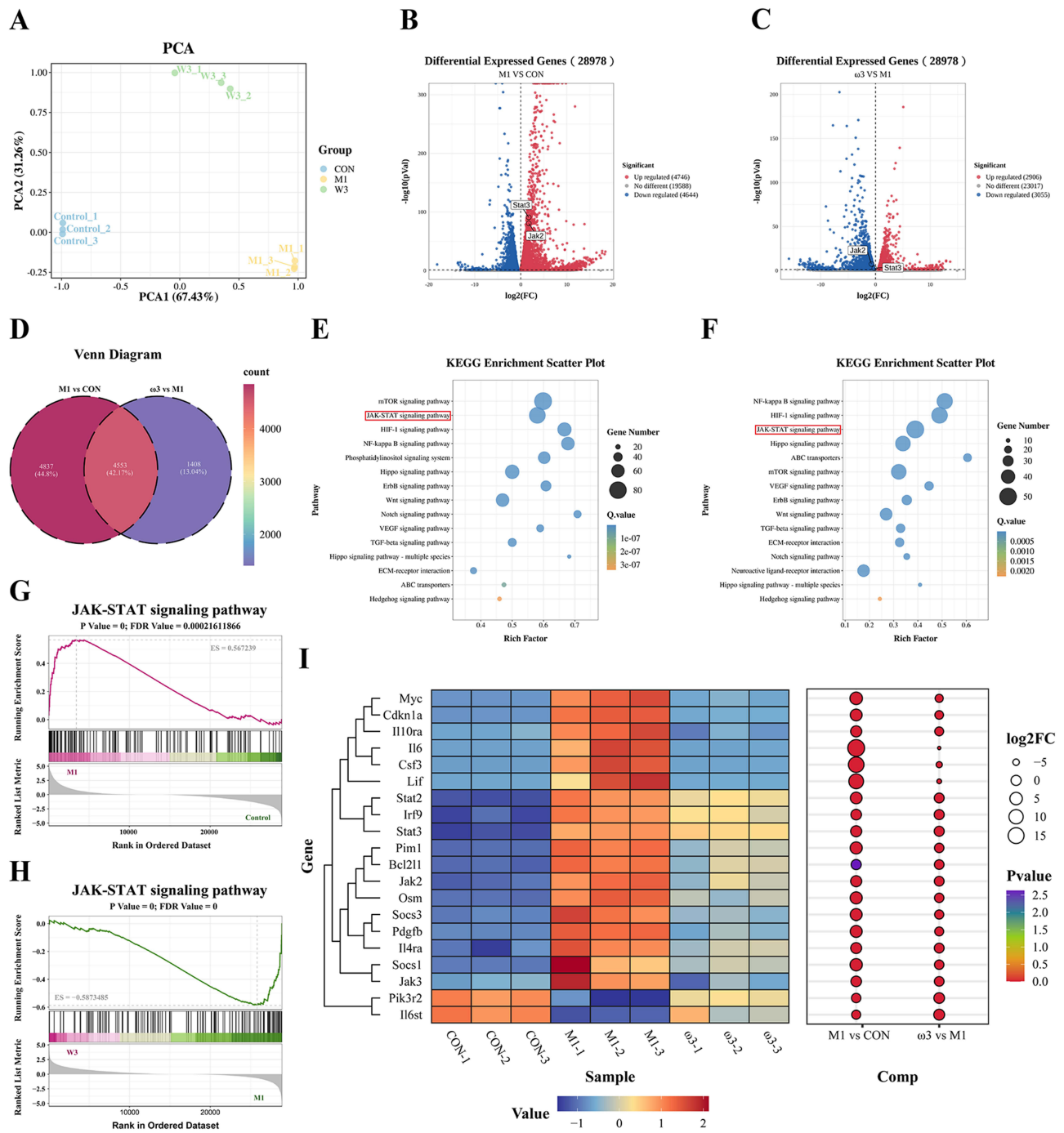


Figure 4 ω -3 PUFAs inhibit M1 macrophage polarization through the JAK2/STAT3 signaling pathway. **(A)** PCA plot of CON, M1, and ω 3 treated samples. **(B and C)** Volcano plots of up-regulated and down-regulated differentially expressed genes between M1 vs CON group and ω 3 vs M1 group. **(D)** Venn diagram of M1 vs CON group and ω 3 vs M1 group. **(E and F)** Bubble plots of KEGG enrichment analysis between M1 vs CON group and ω 3 vs M1 group. **(G and H)** GSEA plots of the JAK-STAT signaling pathway for M1 vs CON group and ω 3 vs M1 group. **(I)** Heatmap and bubble plot of genes in the JAK-STAT signaling pathway for the CON, M1, and ω 3 groups.

significantly blunting the inhibitory effects of ω -3 PUFAs on cytokine production (Figure 7E and F). These results further confirm that inhibition of the JAK2/STAT3 signaling pathway is the primary mechanism through which ω -3 PUFAs inhibit M1 polarization and inflammatory responses.

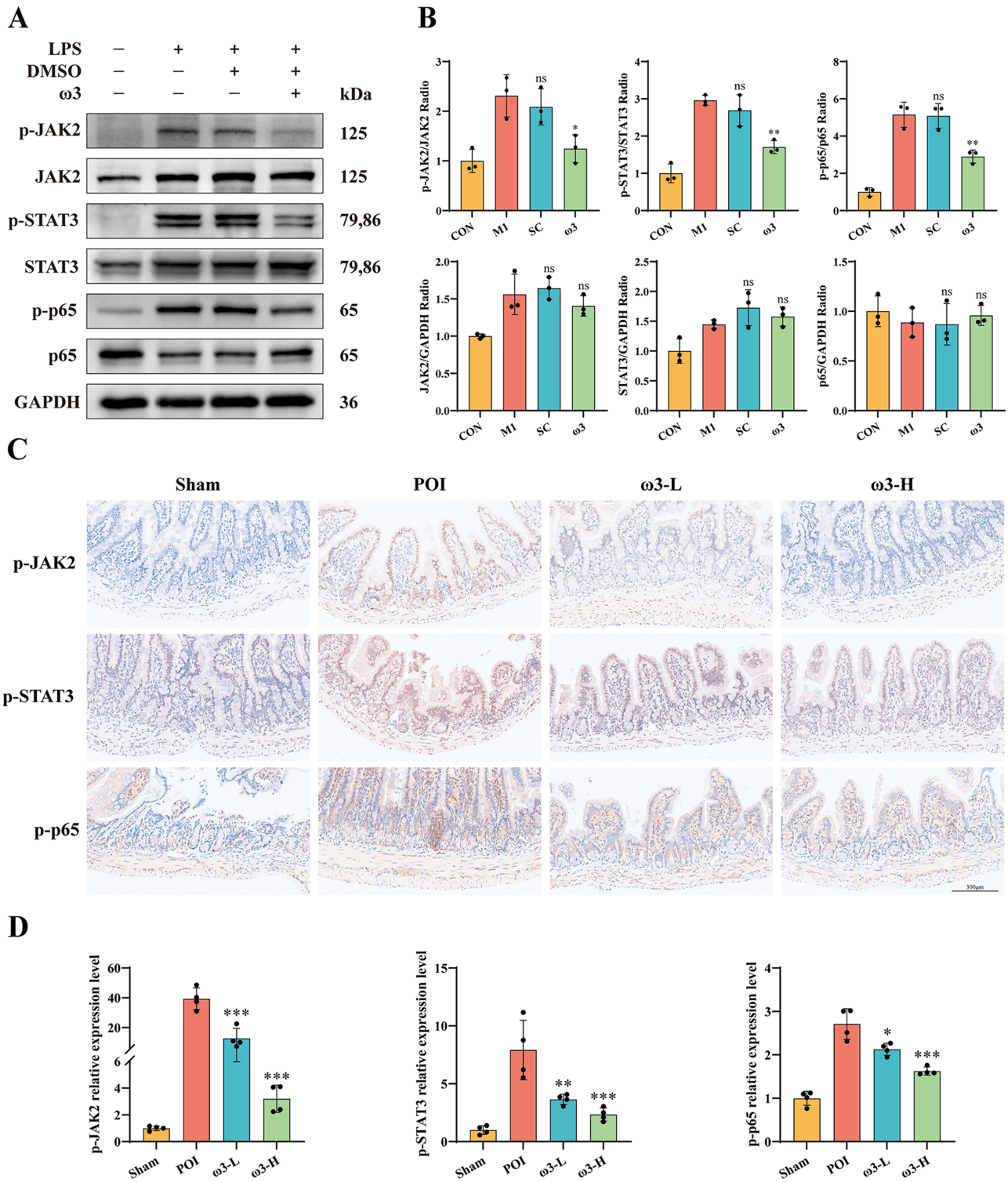


Figure 5 ω -3 PUFAs suppress JAK2/STAT3 signaling activation in macrophages and ileal tissues. **(A and B)** Western blot analysis of p-JAK2, JAK2, p-STAT3, STAT3, p-p65 and p65 protein levels in RAW 264.7 macrophages (n = 3). **(C and D)** IHC staining for p-JAK2, p-STAT3, and p-p65 in ileal tissues (n = 4). Scale bar: 300 μ m. *P < 0.05, **P < 0.01, ***P < 0.001, ns (not significant) vs M1 group (in vitro) or POI group (in vivo).

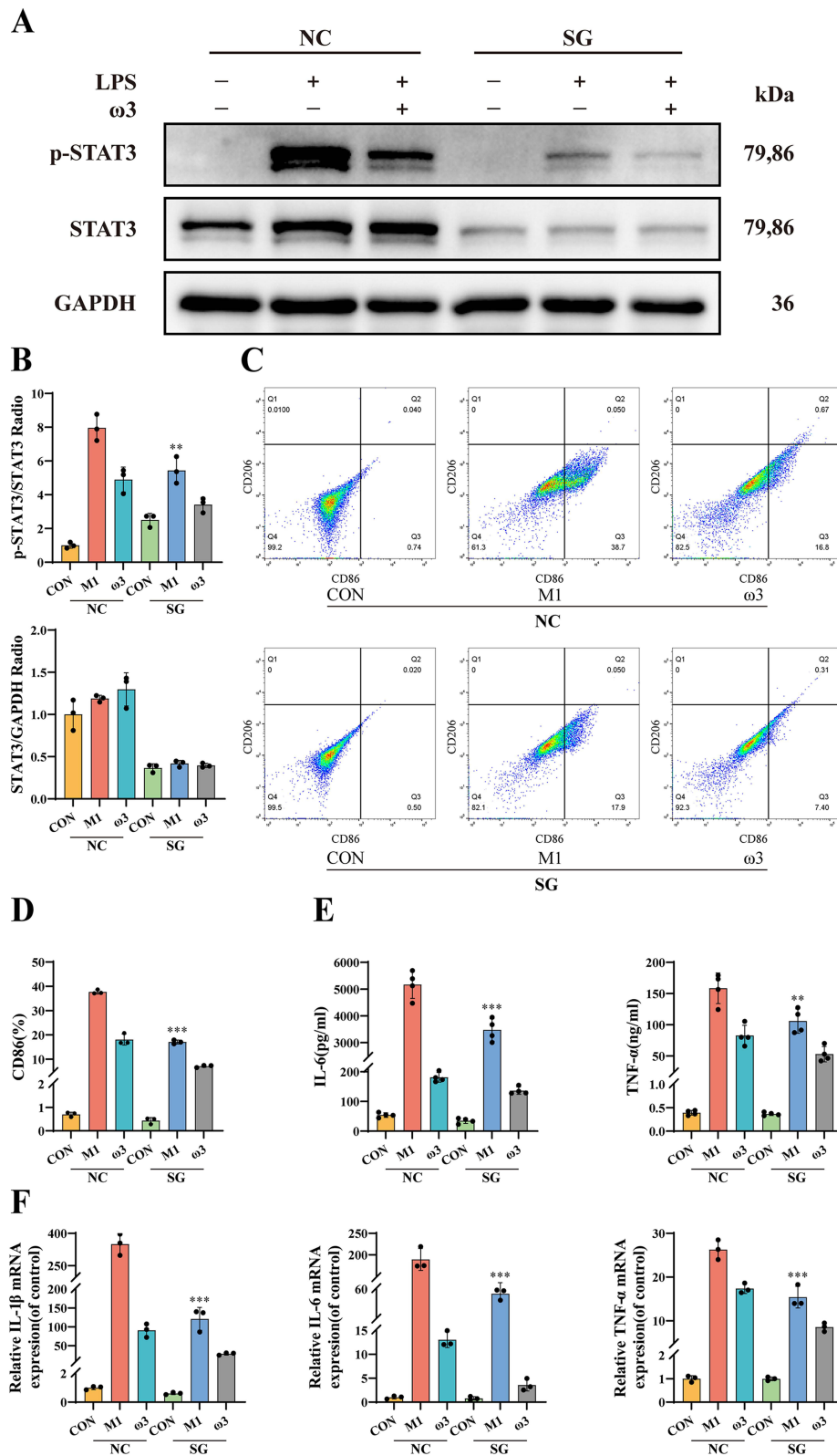


Figure 6 The JAK2/STAT3 signaling pathway regulates M1 macrophage polarization. **(A and B)** Western blot analysis of p-STAT3 in RAW 264.7 macrophages transfected with sg-NC or sg-STAT3 (n = 3). **(C and D)** Flow cytometry analysis of M1 polarization (n = 3). **(E)** Levels of IL-6 and TNF-α in cell supernatants measured by ELISA (n = 4). **(F)** mRNA expression levels of IL-1β, IL-6, and TNF-α determined by qRT-PCR (n = 3). Groups: sg-NC = Non-targeting control; sg-STAT3 = STAT3-knockout. **P < 0.01, ***P < 0.001, vs M1 + sg-NC group.

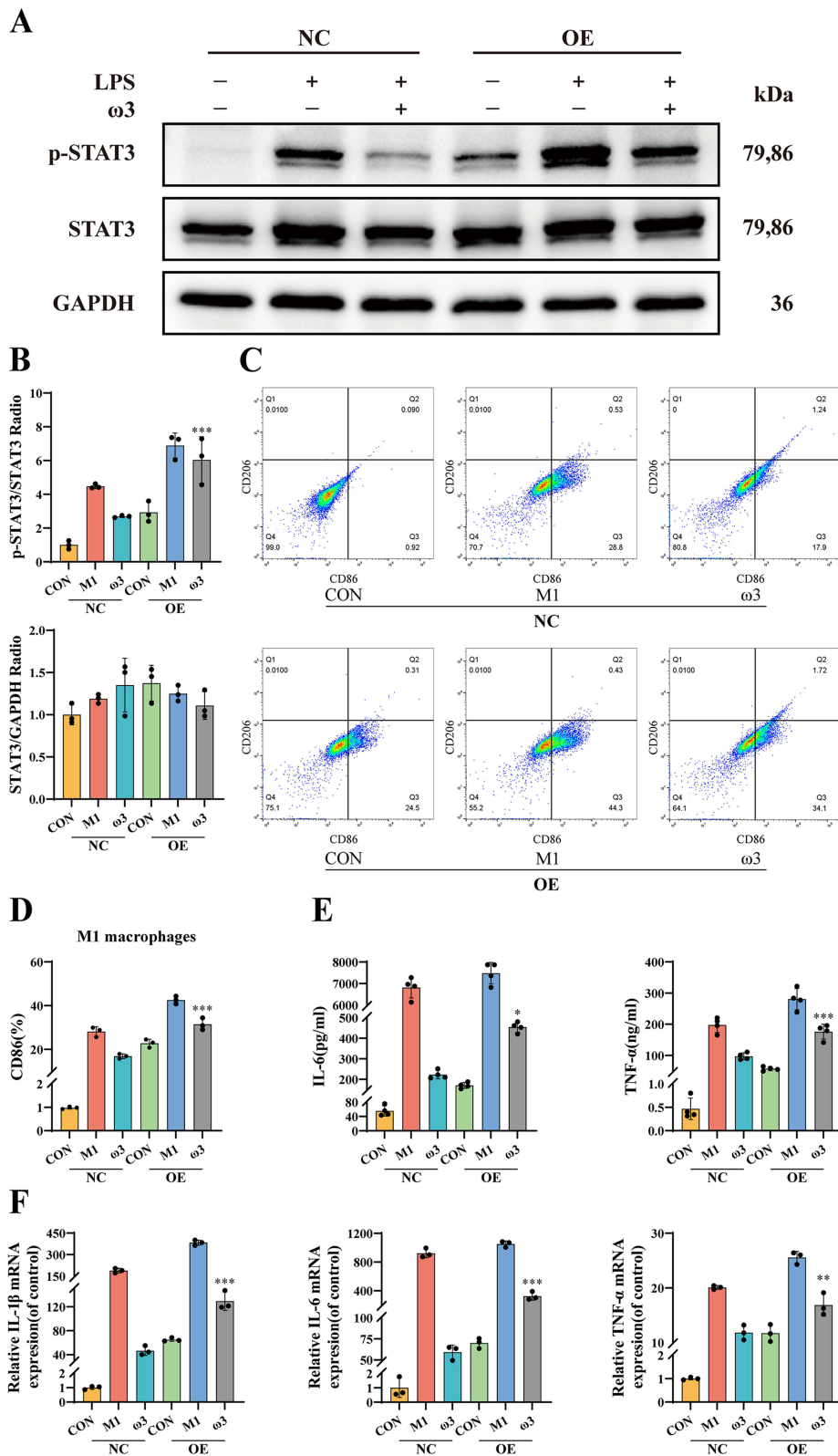


Figure 7 ω-3 PUFAs regulate M1 macrophage polarization through the JAK2/STAT3 signaling pathway. (A and B) Western blot analysis of p-STAT3 in RAW 264.7 macrophages transfected with NC or STAT3-OE (n = 3). (C and D) Flow cytometry analysis of M1 polarization (n = 3). (E) Levels of IL-6 and TNF-α in cell supernatants measured by ELISA (n = 4). (F) mRNA expression levels of IL-1β, IL-6, and TNF-α determined by qRT-PCR (n = 3). Groups: NC = Empty vector control; OE = STAT3-overexpression. *P < 0.05, **P < 0.01, ***P < 0.001 vs ω-3 + NC group.

Discussion

Postoperative ileus (POI) is a frequent postoperative issue occurring after abdominal operations, manifesting as extended impairment of gastrointestinal motility that can delay recovery.²⁶ Consequently, accelerating POI recovery is paramount for improving patient outcomes. Surgical manipulation of the intestine triggers an inflammatory cascade: resident macrophages become activated and secrete substances including nitric oxide and prostaglandins; these compounds directly suppress smooth muscle contractility and play a role in the pathogenesis of POI.^{27–29} Although it has been established that ω -3 PUFAs and their metabolites exhibit anti-inflammatory properties and enhance intestinal barrier integrity in the context of POI,^{30–32} the precise mechanisms have not been fully understood.

Based on our prior clinical data, early enteral supplementation with ω -3 PUFAs after colorectal surgery protects vagal function and reduces intestinal inflammation, thereby accelerating gastrointestinal recovery—as reflected in the faster return of bowel sounds and shorter time to first flatus/defecation—and delaying the onset and progression of POI.^{24,33} In a mouse model, ω -3 PUFA administration significantly improved gastrointestinal transit in the charcoal test and reduced ileal tissue damage and inflammatory cell infiltration. Importantly, we found that intestinal macrophages – key drivers of POI^{13,14} – were decreased markedly in ω -3-treated mice. This decline in macrophage infiltration correlated with a dose-dependent reduction in the expression of key pro-inflammatory cytokines (IL-1 β , IL-6, TNF- α) within ileal tissues, observed at both transcriptional and translational levels. These data indicate that ω -3 PUFAs mitigate intestinal inflammation in POI, at least in part, by limiting macrophage recruitment and activation.

Macrophage polarization plays a pivotal role in regulating inflammatory responses. Following intestinal injury, infiltrating macrophages rapidly polarize toward the pro-inflammatory M1 phenotype, secreting cytokines and reactive oxygen species that contribute to further tissue injury.^{13,14,34} EPA and DHA, the active components of ω -3 PUFAs, have been implicated in modulating macrophage polarization through effects on lipid and energy metabolism.^{35,36} Consistent with this, our *in vitro* experiments showed that ω -3 PUFAs effectively suppressed LPS + IFN- γ -induced M1 polarization of RAW 264.7 cells, reducing the proportion of CD86⁺ macrophages. This shift was accompanied by a significant reduction in expression and secretion of hallmark M1 cytokines (IL-1 β , IL-6, TNF- α), reinforcing the concept that ω -3 PUFAs reprogram macrophages toward a less inflammatory state.

We performed RNA-seq to elucidate the underlying molecular mechanism. This analysis revealed a profound effect of ω -3 PUFAs on the macrophage transcriptome, with specific downregulation of genes associated with the JAK/STAT signaling pathway in M1-polarized cells. The JAK/STAT pathway is a well-established regulator of macrophage activation.¹⁶ External stimuli trigger JAK2 phosphorylation and subsequent STAT3 activation, directly driving M1 polarization and inflammatory cytokine production.¹⁸ Accordingly, we investigated this pathway. Our Western blot and immunohistochemical analyses provided definitive evidence: ω -3 PUFA treatment significantly suppressed phosphorylation (activation) of JAK2, STAT3, and the downstream NF- κ B subunit p65, both in LPS + IFN- γ -stimulated macrophages *in vitro* and the inflamed ileum of POI mice *in vivo*. These data strongly suggest that inhibition of the JAK2/STAT3/NF- κ B signaling axis is a central mechanism by which ω -3 PUFAs modulate macrophage polarization and dampen intestinal inflammation, ultimately improving POI.

To establish causality, we manipulated STAT3 genetically. STAT3 knockout alone inhibited M1 polarization and cytokine production; strikingly, STAT3 knockout synergized with ω -3 PUFA treatment to nearly abolish M1 markers and inflammatory mediators. Conversely, STAT3 overexpression enhanced M1 polarization and cytokine secretion and critically attenuated the suppressive effects of ω -3 PUFAs on these parameters. These complementary genetic approaches provide conclusive evidence that STAT3 is a critical downstream effector mediating the anti-inflammatory actions of ω -3 PUFAs in macrophages. They demonstrate that ω -3 PUFAs exert their protective effects primarily by suppressing the JAK2/STAT3 pathway.

Our findings identify JAK2/STAT3 signaling as a novel mechanistic target for ω -3 PUFAs in intestinal inflammation and POI. Previous reports have implicated other pathways in the anti-inflammatory effects of ω -3 PUFAs, such as inhibition of MAPK and NF- κ B or activation of PPAR γ .^{37–40} It is likely that ω -3 PUFAs act on multiple targets, yielding synergistic anti-inflammatory effects. Several limitations of this study should be noted. Although our key findings were validated *in vivo*, the mechanistic analyses were primarily restricted to macrophages, without examining other POI-relevant immune cells, such as mast cells and neutrophils. Additionally, the inflammasome adaptor ASC is absent in RAW 264.7 cells, which may explain the

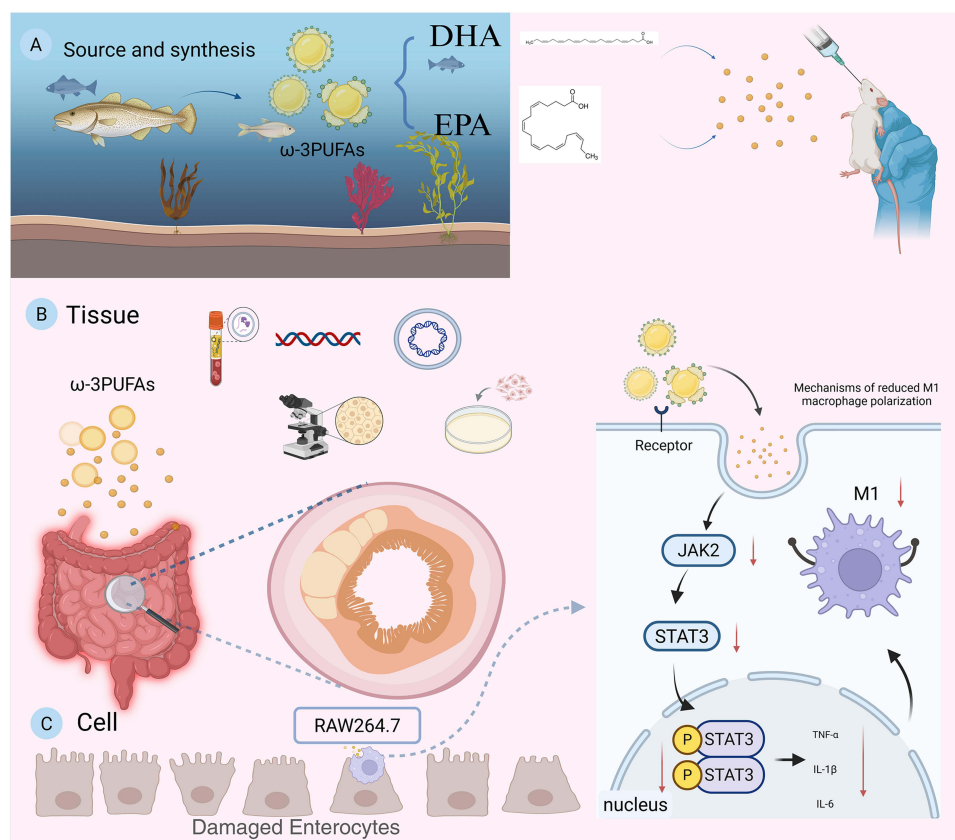


Figure 8 The illustration of the mechanisms for ω -3 PUFAs in the treatment of POI. **(A)** Source, Extraction, and Administration of ω -3 PUFAs: ω -3 PUFAs, primarily comprising EPA and DHA, were extracted into an oil form and administered to mice via oral gavage. **(B)** Tissue-Level Mechanism of Action of ω -3 PUFAs: ω -3 PUFAs exert their therapeutic effects within the inflamed ileum, mitigating POI by reducing macrophage infiltration. **(C)** Cellular-Level Mechanism of Action of ω -3 PUFAs: ω -3 PUFAs suppress M1 macrophage polarization and subsequent pro-inflammatory cytokine release through inhibition of the JAK2/STAT3 signaling pathway within macrophages. The figure is created by <https://www.biorender.com>.

detection of IL-1 β mRNA but not mature protein in vitro, potentially underestimating ω -3 PUFA effects on this cytokine.⁴¹ The precise interaction between ω -3 PUFAs (or their metabolites) and the JAK2/STAT3 pathway, as well as their crosstalk with other targets, also remains to be defined. Furthermore, our study focused only on the acute phase of POI, leaving longer-term effects unexplored. Future work should therefore expand to broader immune populations, employ myeloid-specific STAT3 knockout models to clarify pathway mechanisms, and conduct translational studies to determine optimal dosing and evaluate long-term efficacy in POI patients.

Conclusion

Our findings demonstrate that ω -3 PUFAs alleviate POI through inhibition of the JAK2/STAT3 signaling pathway within intestinal macrophages. This intervention redirects macrophage polarization from the pro-inflammatory M1 phenotype, thereby attenuating local inflammatory responses and maintaining normal intestinal function. By reducing inflammatory injury to the intestinal barrier, ω -3 PUFAs promote the restoration of postoperative gastrointestinal motility. These results support the potential of ω -3 PUFAs as a preventive or therapeutic agent for POI (Figure 8A–C).

Data Sharing Statement

The data used to support this study's findings are available from the corresponding author upon request.

Acknowledgments

We would like to express our sincere gratitude to Dr. G. Wang and Dr. Z.W. Jiang for their valuable comments, which have greatly improved this paper. The mechanism diagram in this study was created using BioRender, and we sincerely appreciate the platform's support.

Author Contributions

Xuan Zhao and Jing Yu contributed equally to this work and share first authorship. Xuan Zhao: Data curation, Formal Analysis, Investigation, Methodology, Visualization, Writing - original draft. Jing Yu: Formal Analysis, Investigation, Methodology, Writing - review & editing. Tianle Zhang: Data curation, Methodology, Writing - review & editing. Yufei Zhang: Data curation, Methodology, Writing - review & editing. Liuchuang Zhang: Investigation, Visualization, Writing - review & editing. Ye Wang: Investigation, Visualization, Writing - review & editing. Chen Yi: Investigation, Visualization, Writing - review & editing. Huafeng Pan: Formal Analysis, Investigation, Writing - review & editing. Haifeng Wang: Formal Analysis, Investigation, Writing - review & editing. Miaomiao Ge: Formal Analysis, Investigation, Writing - review & editing. Zhiwei Jiang: Conceptualization, Funding acquisition, Supervision, Validation, Writing - review & editing. Gang Wang: Conceptualization, Funding acquisition, Supervision, Validation, Writing - review & editing. All authors gave final approval of the version to be published; have agreed on the journal to which the article has been submitted; and agree to be accountable for all aspects of the work.

Funding

This work was supported by the Jiangsu Provincial Key Discipline Project (ZDXK202251), Jiangsu Provincial Association of Chinese Medicine Revitalization and Development Project (ZXFZ2024001), and Jiangsu Postgraduate Research Innovation Program (KYCX25_2279).

Disclosure

The authors declare that there is no conflict of interest in this work.

References

- Hedrick TL, McEvoy MD, Mythen MMG, et al. American society for enhanced recovery and perioperative quality initiative joint consensus statement on postoperative gastrointestinal dysfunction within an enhanced recovery pathway for elective colorectal surgery. *Anesth. Analg.* 2018;126:1896–1907. doi:10.1213/ANE.0000000000002742
- Mazzotta E, Villalobos-Hernandez EC, Fiorda-Diaz J, Harzman A, Christofi FL. Postoperative ileus and postoperative gastrointestinal tract dysfunction: pathogenic mechanisms and novel treatment strategies beyond colorectal enhanced recovery after surgery protocols. *Front Pharmacol.* 2020;11:583422. doi:10.3389/fphar.2020.583422
- Harnsberger CR, Maykel JA, Alavi K. Postoperative ileus. *Clin. Colon Rectal Surg.* 2019;32:166–170. doi:10.1055/s-0038-1677003
- Xu P, Wang G, Jiang Z. Research advances in assessment and prevention of postoperative ileus. *Zhejiang J Integr Tradit Chin West Med.* 2024;34:679–682.
- Nan H, Wang G, Jiang Z, Wang H. Early exploration and practice of enhanced recovery after surgery in China. *J Eras.* 2024;7:29–35.
- Iskander O. An outline of the management and prevention of postoperative ileus: a review. *Medicine.* 2024;103(24):e38177. PMID: 38875379; PMCID: PMC11175850. doi:10.1097/MD.00000000000038177
- McKechnie T, Tessier L, Archer V, et al. Enhanced recovery after surgery protocols following emergency intra-abdominal surgery: a systematic review and meta-analysis. *Eur J Trauma Emerg Surg off Publ Eur Trauma Soc.* 2024;50:679–704. doi:10.1007/s00068-023-02387-6
- Namba Y, Hirata Y, Mukai S, et al. Clinical indicators for the incidence of postoperative ileus after elective surgery for colorectal cancer. *BMC Surg.* 2021;21:80. doi:10.1186/s12893-021-01093-7
- Venara A, Neunlist M, Slim K, et al. Postoperative ileus: pathophysiology, incidence, and prevention. *J Visc Surg.* 2016;153:439–446. doi:10.1016/j.jviscsurg.2016.08.010
- Mao H, Milne TGE, O'Grady G, Vather R, Edlin R, Bissett I. Prolonged postoperative ileus significantly increases the cost of inpatient stay for patients undergoing elective colorectal surgery: results of a multivariate analysis of prospective data at a single institution. *Dis Colon Rectum.* 2019;62:631–637. doi:10.1097/DCR.0000000000001301
- Hussain Z, Park H. Inflammation and impaired gut physiology in post-operative ileus: mechanisms and the treatment options. *J Neurogastroenterol Motil.* 2022;28:517–530. doi:10.5056/jnm22100
- Boeckstaens GE, de Jonge WJ. Neuroimmune mechanisms in postoperative ileus. *Gut.* 2009;58:1300–1311. doi:10.1136/gut.2008.169250
- Asano K, Takahashi N, Ushiki M, et al. Intestinal CD169(+) macrophages initiate mucosal inflammation by secreting CCL8 that recruits inflammatory monocytes. *Nat Commun.* 2015;6:7802. doi:10.1038/ncomms8802
- Buscaill E, Deraison C. Postoperative ileus: a pharmacological perspective. *Br. J Pharmacol.* 2022;179:3283–3305.

15. Cai Y, Li H, Nan H, et al. Randomized trial on electroacupuncture for recovery of postoperative gastrointestinal function based on long-term monitoring device. *Ann Surg Oncol*. 2025;32:5165–5172. doi:10.1245/s10434-025-17239-3
16. Yan Y, Zhang L-B, Ma R, et al. Jolkinolide B ameliorates rheumatoid arthritis by regulating the JAK2/STAT3 signaling pathway. *Phytomedicine Int J Phytother Phytopharm*. 2024;124:155311.
17. Li L, Xu T, Huang C, Peng Y, Li J. NLRP5 mediates cytokine secretion in RAW2647 macrophages and modulated by the JAK2/STAT3 pathway. *Inflammation*. 2014;37:835–847. doi:10.1007/s10753-013-9804-y
18. Wang F, Zhang S, Jeon R, et al. Interferon gamma induces reversible metabolic reprogramming of M1 macrophages to sustain cell viability and pro-inflammatory activity. *Ebiomedicine*. 2018;30:303–316. doi:10.1016/j.ebiom.2018.02.009
19. D'Angelo S, Motti ML, Meccariello R. Meccariello, ω -3 and ω -6 polyunsaturated fatty acids, obesity and cancer. *Nutrients*. 2020;12:2751. doi:10.3390/nu12092751
20. Spooner MH, Jump DB. Nonalcoholic fatty liver disease and omega-3 fatty acids: mechanisms and clinical use. *Annu Rev Nutr*. 2023;43:199–223. doi:10.1146/annurev-nutr-061021-030223
21. Yan D, Hou Y, Lei X, et al. The impact of polyunsaturated fatty acids in cancer and therapeutic strategies. *Curr Nutr Rep*. 2025;14:46. doi:10.1007/s13668-025-00639-y
22. Liu L, Guo H, Song A, et al. Progranulin inhibits LPS-induced macrophage M1 polarization via NF- κ B and MAPK pathways. *BMC Immunol*. 2020;21(1):32. doi:10.1186/s12865-020-00355-y
23. Gutiérrez S, Svahn SL, Johansson ME. Effects of omega-3 fatty acids on immune cells. *Int J Mol Sci*. 2019;20:5028. doi:10.3390/ijms20205028
24. Wang G, Xu P, Zhao X, et al. Effect of ω -3 polyunsaturated fatty acids on recovery of autonomic nervous system and intestinal function after laparoscopic colorectal cancer surgery. *J Shandong Univ*. 2025;63:36–42.
25. Wang G, Cai Y, Wang Y, et al. The impact of ω -3 polyunsaturated fatty acids on the recovery of autonomic nervous and intestinal functions following robot-assisted gastrectomy. *Yixue Xinzhi Zazhi*. 2025;35(7):783–790.
26. Alkan S, Cakir M, Sentiurk M, Varman A, Duyan AG. The efficacy and results of medical treatment in postoperative ileus. *Niger J Clin Pract*. 2023;26:497–501. doi:10.4103/njcp.njcp_618_22
27. Enderes J, Malleš S, Schneider R, et al. A population of radio-resistant macrophages in the deep myenteric plexus contributes to postoperative ileus via toll-like receptor 3 signaling. *Front Immunol*. 2020;11:581111. doi:10.3389/fimmu.2020.581111
28. Y T, F H, M F, et al. Neuronal stimulation with 5-hydroxytryptamine 4 receptor induces anti-inflammatory actions via α 7nACh receptors on muscularis macrophages associated with postoperative ileus. *Gut*. 2011;60.
29. Malleš S, Schneider R, Schneiker B, et al. Sympathetic denervation alters the inflammatory response of resident muscularis macrophages upon surgical trauma and ameliorates postoperative ileus in mice. *Int J Mol Sci*. 2021;22:6872. doi:10.3390/ijms22136872
30. Yi K, An L, Qi Y, et al. Docosahexaenoic acid (DHA) promotes recovery from postoperative ileus and the repair of the injured intestinal barrier through mast cell-nerve crosstalk. *Int Immunopharmacol*. 2024;136:112316. doi:10.1016/j.intimp.2024.112316
31. Moore BA. Editorial: preventing postoperative ileus with n-3 PUFA. *J Leukoc Biol*. 2016;99:225–227. doi:10.1189/jlb.3CE0815-341R
32. Wehner S, Meder K, Vilz TO, et al. Preoperative short-term parenteral administration of polyunsaturated fatty acids ameliorates intestinal inflammation and postoperative ileus in rodents. *Langenbecks Arch. Surg*. 2012;397:307–315.
33. Pei L, Wang G, Yang S, et al. Electroacupuncture reduces duration of postoperative ileus after laparoscopic gastrectomy for gastric cancer: a multicenter randomized trial. *Gastroenterology*. 2025;S0016-5085(25):373–377.
34. Docsa T, Bhattarai D, Sipos A, Wade CE, Cox CS, Uray K. CXCL1 is upregulated during the development of ileus resulting in decreased intestinal contractile activity. *Neurogastroenterol. Motil*. 2020;32:e13757.
35. Pawłowska-Kamieniak A, Krawiec P, Pac-Kożuchowska E. Interleukin 6: biological significance and role in inflammatory bowel diseases. *Adv Clin Exp Med off Organ Wrocław Med Univ*. 2021;30:465–469. doi:10.17219/acem/130356
36. Neurath MF. IL-23 in inflammatory bowel diseases and colon cancer. *Cytokine Growth Factor Rev*. 2019;45:1–8. doi:10.1016/j.cytogfr.2018.12.002
37. Kuda O, Rossmeisl M, Kopecky J. Omega-3 fatty acids and adipose tissue biology. *Mol Aspects Med*. 2018;64:147–160. doi:10.1016/j.mam.2018.01.004
38. Graf D, Weitkunat K, Dötsch A, et al. Specific wheat fractions influence hepatic fat metabolism in diet-induced obese mice. *Nutrients*. 2019;11:2348. doi:10.3390/nu11102348
39. Calder PC. Marine omega-3 fatty acids and inflammatory processes: effects, mechanisms and clinical relevance. *Biochim. Biophys. Acta*. 2015;1851:469–484. doi:10.1016/j.bbali.2014.08.010
40. Chang HY, Lee H-N, Kim W, Surh Y-J. Docosahexaenoic acid induces M2 macrophage polarization through peroxisome proliferator-activated receptor γ activation. *Life Sci*. 2015;120:39–47. doi:10.1016/j.lfs.2014.10.014
41. Watanabe N, Tamai R, Kiyoura Y. Alendronate augments lipid a-induced IL-1 β release by ASC-deficient RAW264 cells via AP-1 activation. *Exp Ther Med*. 2023;26:577. doi:10.3892/etm.2023.12276